Comparison of Dynamical Heterogeneity in Hard-Sphere and Attractive Glass Formers

David R. Reichman
Department of Chemistry, Columbia University, 3000 Broadway, New York, NY 10027

Eran Rabani
School of Chemistry, The Sackler Faculty of Exact Sciences, Tel Aviv University, Tel Aviv 69978, Israel

Phillip L. Geissler
Department of Chemistry, University of California, and Physical Biosciences and Materials Sciences Divisions, Lawrence Berkeley National Laboratory, Berkeley, CA 94720

(Dated: February 2, 2008)

Using molecular dynamics simulations, we have determined that the nature of dynamical heterogeneity in jammed liquids is very sensitive to short-ranged attractions. Weakly attractive systems differ little from dense hard-sphere and Lennard-Jones fluids: Particle motion is punctuated and tends to proceed in steps of roughly a single particle diameter. Both of these basic features change in the presence of appreciable attractions. Transient periods of particle mobility and immobility cannot be discerned at intermediate attraction strength, for which structural relaxation is greatly enhanced. Strong attractions, known to dramatically inhibit relaxation, restore bimodality of particle motion. But in this regime, transiently mobile particles move in steps that are significantly more biased toward large displacements than in the case of weak attractions. This modified feature of dynamic heterogeneity, which cannot be captured by conventional mode coupling theory, verifies recent predictions from a model of spatially correlated facilitating defects.

Dynamical heterogeneity is perhaps the most revealing feature of relaxation in deeply supercooled liquids. A high-temperature fluid is dynamically homogeneous in the sense that the local environment restricting fluctuations of any given particle is, for all important purposes, identical to that surrounding any other particle, even on the short time scales of basic microscopic motions. The distribution $P(\delta\mathbf{r}, t)$ of particle displacements $\delta\mathbf{r}$ as a function of time t provides a quantitative measure of such uniformity. Results of molecular dynamics simulations indicate that $P(\delta\mathbf{r}, t)$ is Gaussian over a wide range of displacements, as would be expected from a mean-field perspective, for typical dense fluids[1]. The microscopic environments constraining particle motion in a glassy material are by contrast profoundly nonuniform, even on the long time scales of large-wavelength relaxation[2, 3, 4, 5]. This fact has been clearly demonstrated by experiments that focus on dynamics of single probe molecules[6] or subsets of molecules in a pure liquid that relax more slowly than the average[7, 8]. As a result, $P(\delta\mathbf{r}, t)$ develops substantial weight in the wings, reflected in appreciably nonzero values of the non-Gaussian parameter $\alpha_2(t) = \frac{3}{5}\langle\delta r^4(t)\rangle/\langle\delta r^2(t)\rangle^2 - 1$. Microscopy studies of colloidal suspensions have confirmed this expectation[9].

Through extensive computer simulations, a detailed picture of dynamical heterogeneity in simple jammed liquids (e.g., a binary mixture of Lennard-Jones spheres) has developed[10]. At low temperatures, the majority of particles are confined within cages, composed of neighboring particles, that may persist for very long times. Eventually, a rare, collective rearrangement frees a particle from its cage, transiently allowing it to move rapidly over distances comparable to a particle diameter. Since such a displacement itself facilitates local rearrangement, transient mobility appears to propagate continuously and with some degree of directionality. Schematic models of glassiness have been constructed with only these features in mind[11, 12, 13]. They account for a surprising variety of anomalous behaviors and yield unique scaling predictions for the length and time scales characterizing relaxation[13, 14, 15].

These basic features of dynamical heterogeneity have little to do with the identity of particles comprising a glassy material or with the interactions between them. They have been reported for many model atomic liquids as well as for viscous silica, a network-forming liquid which vitrifies with qualitatively different temperature dependence[16]. It is therefore tempting to presume that the scenario sketched above is universal among supercooled molecular liquids[12, 17].

When interactions between particles in a simple liquid are augmented by strong, short-ranged attractions, spatially averaged dynamical quantities change in nontrivial ways[18, 19, 20, 21]. This situation has been realized experimentally by adding linear chain molecules to suspensions of colloidal particles, whose direct interactions are almost purely repulsive[22]. By varying $\phi_{\rm p}$ one can tune the fluid from purely repulsive to strongly attractive. For large colloid volume fraction, $\phi_{\rm c}$, and vanishing attraction strength ($\phi_{\rm p} = 0$), the suspension is in essence

a dense hard-sphere fluid with the basic phenomenology of simple supercooled liquids. As ϕ_p increases, however, relaxation accelerates significantly, so that a hard-sphere glass can be "melted" by adding attractions[18]. Beyond a certain value of ϕ_p, relaxation becomes instead more sluggish as more polymer is added, leading to revitrification at large ϕ_p.

In this paper we examine whether the peculiar behavior of attractive colloids reflects fundamental changes in the nature of dynamical heterogeneity. Although extensive computational work has been done to characterize such heterogeneity in simple liquids, previous simulations of materials with short-ranged attractions have not focused on correlated microscopic motions. For this purpose we have adopted the model of Puertas *et al.* for polymer-mediated interactions between colloids[19, 20]. The effective interaction potential between a pair of colloids separated by distance r, described in detail in Refs. 21-22, is plotted in Fig. 1 for the values of ϕ_p we have studied. Interactions consist of a short-ranged repulsion parameterized by the sum of particle radii, a short-ranged attraction that mimics the polymer-induced depletion interaction, and a slowly varying, long-ranged repulsion designed to prohibit phase separation [23]. The effective range and form of each term are precisely as given in Refs. 21-22. We have focused on weakly polydisperse systems, in which these radii are drawn from a uniform distribution, $p(R) = (2\,\delta a)^{-1}\theta[R-(a-\delta a)]\theta[(a+\delta a)-R]$, with mean a and half-width $\delta a = a/10$. The Heaviside funcion $\theta(x)$ is defined as usual to be 1 for $x \geq 0$, and 0 for $x < 0$. In this paper all quantities with units of length have been scaled by the mean *radius* a, and quantities with units of time have been scaled by $t_0 = \sqrt{\frac{8a^2}{3T}}$. We have used standard methods of molecular dynamics to propagate equilibrated systems of 1000 periodically replicated colloidal particles, stochastically rescaling colloid momenta every 101 time steps to maintain a Boltzmann distribution at temperature $T = \frac{4}{3}$. We have investigated a single colloid volume fraction $\phi_c = \frac{4\pi N}{3V}a^3(1+(\delta a/a)^2) = 0.55$ and several polymer volume fractions (i.e., attraction strengths as plotted in Fig. 1) ranging from $\phi_p = 0.05$ to $\phi_p = 0.375$.

In order to contrast features of dynamic heterogeneity unique to attractive systems with those generic to simple supercooled liquids, we have selected a colloid density for which relaxation is already very slow for $\phi_p = 0$. The self-diffusion constant $D(\phi_p)$, plotted in Fig. 1 as a function of ϕ_p, thus evinces the re-entrant behavior we have described. Specifically, D increases by two orders of magnitude as ϕ_p approaches 0.25 and then decreases sharply for higher polymer concentrations. Any meaningful comparison of relaxation mechanisms at different ϕ_p must take into account the disparate time scales corresponding to this range of diffusivity. Here we examine time evolution over intervals scaled such that the overall

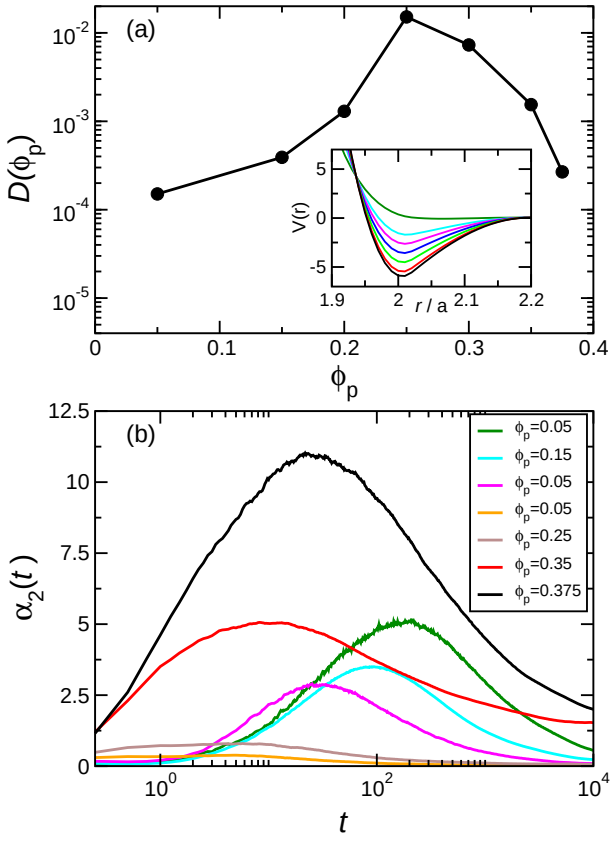

FIG. 1: (a) Diffusion constant D as a function of polymer volume fraction ϕ_p. In each case, D was computed from the mean squared displacement averaged over particle size. Inset: Potential energy of interaction $V(r)$ as a function of the distance r between two particles with radius a for the values of ϕ_p we have studied numerically. From the least negative minimum of $V(r)$ to the most negative minimum, these values are $\phi_p = 0.05$, 0.15, 0.2, 0.25, 0.3, 0.35, and 0.375. (b) Non-Gaussian parameter $\alpha_2(t)$ as a function of time t.

extent of relaxation is comparable for each state. We use several different measures of the extent of relaxation, including $\alpha_2(t)$, mean squared particle displacement, and the dynamic structure factor. Although these choices are somewhat arbitrary, they paint a consistent picture of changes in dynamic heterogeneity induced by short-ranged attractions.

The non-Gaussian parameter, plotted in Fig. 1(b) as a function of time for several values of ϕ_p, indicates that short-ranged attractions effect changes more profound than simply a renormalized average time or length scale[19, 20]. The peak of $\alpha_2(t)$ roughly locates the time of maximum dynamic heterogeneity. We denote the time corresponding to this peak as t^*. The dependence of t^* on ϕ_p closely mirrors that of the diffusion constant, reflecting a global change in relaxation time. But the shape and scale of $\alpha_2(t)$ also change significantly with attraction strength. Most notably, the peak height $\alpha_2(t^*)$ de-

clines by nearly an order of magnitude as ϕ_p approaches 0.25, then grows rapidly for larger values of ϕ_p. This evolution strongly suggests a change in the character of microscopic dynamics[19].

The full distribution of particle displacements, or of their logarithm ($\tilde{P}[\log_{10}(|\delta\mathbf{r}|), t]$), over a specific time interval (of duration t) provides a more detailed picture of microscopic rearrangements[24]. Fig. 2 shows a plot of $\tilde{P}[\log_{10}(|\delta\mathbf{r}|), \tau_0]$ for states representative of weak attractions ($\phi_p = 0.05$), strong attractions ($\phi_p = 0.375$), and intermediate attraction strength ($\phi_p = 0.25$). Since relaxation rates vary greatly among these three states, we have followed Cates et al. [24] in comparing motion over time intervals $\tau_0(\phi_p)$ yielding the same mean squared displacement, $10a^2$. As reflected by $\alpha_2(t)$, the distributions at $\phi_p = 0.05$ and $\phi_p = 0.375$ are highly non-Gaussian, exhibiting distinct populations of especially mobile and especially immobile particles. Cates et al. [24] have reported a similarly bimodal distribution of $\log(|\delta\mathbf{r}|^2)$ for strongly attractive colloids at much lower densities ($\phi_c = 0.4$) and have suggested that such bimodality is a unique feature of attractive glasses. Multi-peaked van Hove distribution functions, however, have been reported several times for systems lacking short-ranged attractions[25, 26, 27]. Indeed, Fig. 2 demonstrates that the distinction between mobile and immobile particles is in fact *more* pronounced when attractions are almost negligibly weak. Bimodally distributed particle displacements thus appear to be a feature common to many sluggish systems.

The glassy states with weak and strong attractions also share a degree of structure in $\tilde{P}[\log_{10}(|\delta\mathbf{r}|), \tau_0]$ within the subpopulation of mobile particles. For $\phi_p = 0.05$ particles clearly tend to move in discrete steps of approximately integer multiples of a typical particle diameter, $2a$. This feature highlights the decoupling of diffusion and structural relaxation in jammed liquids. Although fluctuations in local environment may permit a particle to move out of its cage, density correlations persist such that the newly formed cage has a well-defined spatial relationship with the original. Stepwise motion is much less pronounced at high ϕ_p.

By contrast, the shape of $\tilde{P}[\log_{10}|\delta\mathbf{r}|, \tau_0]$ at $\phi_p = 0.25$ is nearly that of a Gaussian, plotted for reference in Fig. 2. There is evidence neither of a distinct population of immobile particles nor of stepwise motion. The statistics of single-particle displacements at intermediate attraction strength thus more strongly resemble those of a dynamically homogeneous fluid at lower density than those of a non-attractive fluid at the same density. The simplest conclusion is that the $\phi_p = 0.25$ system is in essence dynamically uniform. Evidence exists, however, that correlated motions of neighboring particles do show signs of dynamic heterogeneity[28]. This situation could be expected if particle displacements were dominated by movement of clusters transiently stabilized by

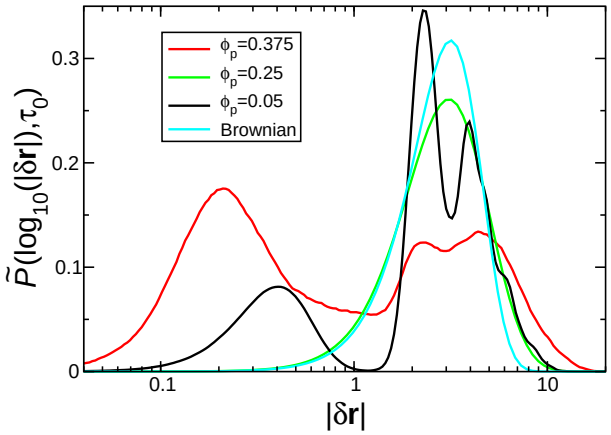

FIG. 2: Distributions $\tilde{P}[\log_{10}|\delta\mathbf{r}|, \tau_0]$ of the logarithm of particle displacements $|\delta\mathbf{r}|$ at time τ_0. Results are shown for polymer volume fractions $\phi_p = 0.05$, 0.375, and 0.25, and for a Gaussian distribution of $\delta\mathbf{r}$. Times $\tau_0(\phi)$ and the width of the reference distribution were chosen to obtain a consistent mean squared displacement, $\langle|\delta\mathbf{r}|^2\rangle = 10a^2$.

attractions[28]. Heterogeneity associated with formation and decay of a cluster would not have a strong signature in $\tilde{P}[\log_{10}|\delta\mathbf{r}|, \tau_0]$ due to translation of the cluster as a whole.

The essence of a dynamic heterogeneity perspective on glassy liquids is that relaxation over any short interval is driven by a small subset of particles that are temporarily much more mobile than the average. The statistics of extreme displacements should therefore be revealing of basic relaxation mechanisms[10]. Here we focus on particles among the 5% most mobile over an interval of length $t^* \ll \tau_0$. We judge mobility in this case by monitoring the largest displacement $|\delta\mathbf{r}|_{max}$ of a particle from its position at the beginning of each interval. Distributions of maximum displacement magnitudes for these especially mobile particles, $P^{(>)}(|\delta\mathbf{r}|_{max}, t^*)$, are plotted in Fig. 3 for each of the polymer volume fractions we have studied. For purposes of comparison, we have scaled $|\delta\mathbf{r}|_{max}$ by its most likely value $r_0(\phi_p)$ for each ϕ_p.

For reference we have included in Fig. 3 an extreme value distribution $\mathcal{P}_B^{(>)}(|\delta\mathbf{r}|)$ that would be obtained for a Brownian analogue of our system. Because maximum displacements are not easily defined for fractal trajectories, we consider in this case the displacement of a particle $|\delta\mathbf{r}|$ from its initial position only at the end of an interval. The interval length is in fact arbitrary, determining only the overall scale of displacements, which is irrelevant for the comparison in Fig. 3. In detail, we computed $\mathcal{P}_B^{(>)}(|\delta\mathbf{r}|)$ by repeatedly drawing $N = 1000$ displacements from a Gaussian distribution with unit variance in all three dimensions, each time adding the $0.05N$ largest values to a histogram. $\mathcal{P}_B^{(>)}(|\delta\mathbf{r}|)$ is therefore a

superposition of extreme value distributions:

$$\mathcal{P}_{\rm B}^{(>)}(|\delta\mathbf{r}|) = \sum_{j=1}^{0.05N} g_j(|\delta\mathbf{r}|).$$

Here, $g_j(|\delta\mathbf{r}|)$ is the probability density for observing $|\delta\mathbf{r}|$ as the $j^{\rm th}$ largest value in a sample of size N. In the limit $N \to \infty$[29],

$$g_j(x) = \frac{j^j}{(j-1)!} \exp\left[j\overline{x}_j(x-\overline{x}) - je^{\overline{x}(x-\overline{x}_j)}\right],$$

where $\overline{x}_j = \sqrt{2\ln(j/N)}$. Because convergence to this asymptotic limit is slow, however, we have chosen to construct $\mathcal{P}_{\rm B}^{(>)}(|\delta\mathbf{r}|)$ from direct sampling.

The scaled distributions in Fig. 3 reveal a monotonic trend toward broadly distributed mobile particle displacements as attraction strength increases. For weak attractions, the large-displacement tail of $P^{(>)}(|\delta\mathbf{r}|_{\rm max}, t^*)$ is attenuated relative to a simple Brownian fluid. For strong attractions, this tail is greatly enhanced. Although the overall shape of the full displacement distribution for intermediate attraction strength is roughly Gaussian, statistics of the extreme subensemble demonstrate that mobile particles nonetheless execute larger jumps (relative to the average) than in a Brownian reference system. This fact is consistent with the attraction-enhanced large-displacement tail of $\tilde{P}[\log_{10}|\delta\mathbf{r}|, \tau_0]$ plotted in Fig. 2.

The comparison in Fig. 3 emphasizes changes in the *shape* of displacement distributions. Because we have scaled distance by different lengths for different values of $\phi_{\rm p}$, these results do not directly imply that transiently mobile particles execute larger jumps in space in the case of strong attractions. They instead reflect the breadth of particle motion relative to the mean, a feature that could reflect tightening of particle cages as well as growth of facilitated regions. More direct evidence for both of these trends is provided by scrutinizing the trajectories of individual particles.

The routes traced by several particles are plotted in Fig. 4 for the smallest and largest values of $\phi_{\rm p}$. We have chosen the duration of displayed trajectories to be τ_α, the time required for correlation of density fluctuations over length scales comparable to a particle diameter to decay by a factor of e. Dynamics over this time scale, which is much larger than t^* in both cases, exhibit the full character of particle motion. This choice also allows a straightforward comparison of dynamics for weak and strong attractions, since the corresponding values of τ_α are very similar ($\tau_\alpha \approx 8 \times 10^3$ for $\phi_{\rm p} = 0.05$ and $\tau_\alpha \approx 10^4$ for $\phi_{\rm p} = 0.375$). The depicted excursions of extremely immobile (top panels of Fig. 4) and extremely mobile (bottom panels) particles reinforce the dynamical features we have gleaned from probability distributions. The 5% least mobile particles exhibit only small flucutations about their initial positions, both for $\phi_{\rm p} = 0.375$ (a)

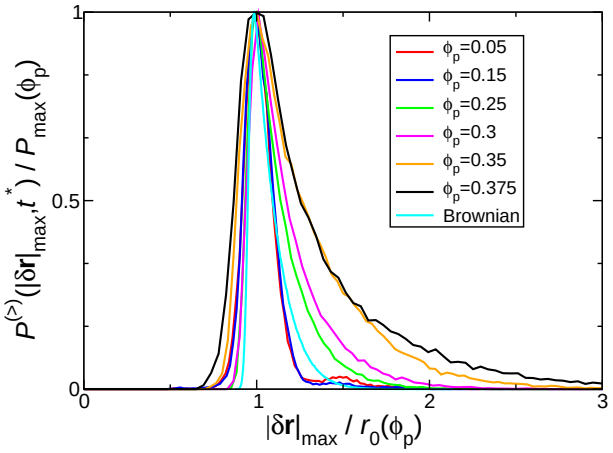

FIG. 3: Distributions $P^{(>)}(|\delta\mathbf{r}|_{\rm max}, t^*)$ of maximum displacements for the 5% most mobile particles. We use as a measure of mobility $|\delta\mathbf{r}|_{\rm max}$, the *largest* displacement a particle undergoes (from its position at time t) during the time interval t to $t + t^*$. Distributions and displacements have been scaled to coincide at the peak of $P^{(>)}$. A scaled extreme displacement distribution is also plotted for a perfectly Brownian system of 1000 particles.

and for $\phi_{\rm p} = 0.05$ (c), even over this long time scale. The cages that constrain these particles' motion are clearly smaller in the case of strong attractions. The 5% most mobile particles, on the other hand, move several particle diameters during the same interval. For the case of weak attractions in panel (d), the discrete nature of particle motion and correlations between subsequent cages are immediately evident. Trajectories are qualitatively different for the case of strong attractions in panel (b). Here, mobile particles explore much more diffuse regions. Domains of facile particle motion are clustered in space and markedly elongated, with asymmetries apparently correlated over several particle radii.

Most of the qualitative changes in dynamical heterogeneity we have reported can be understood as consequences of changing spatial patterns of structural defects[31]. Models based on dynamical heterogeneity typically assume that the subtle defects which enable local relaxation are sufficiently sparse as to be statistically independent (despite significant correlations in defect dynamics). We have proposed that an important effect of short-ranged attractions is to introduce non-negligible spatial correlations among such facilitating entities[30]. In particular, defects should aggregate with increasing attraction strength as an indirect result of particle clustering. Microscopic regions of mobility thus grow in size, but become still more sparse if their overall concentration (loosely analogous to free volume) is held fixed. This picture accounts for the broadening distributions of mobile particle displacements we have computed. Particle trajectories depicted in Fig. 4 make the agreement es-

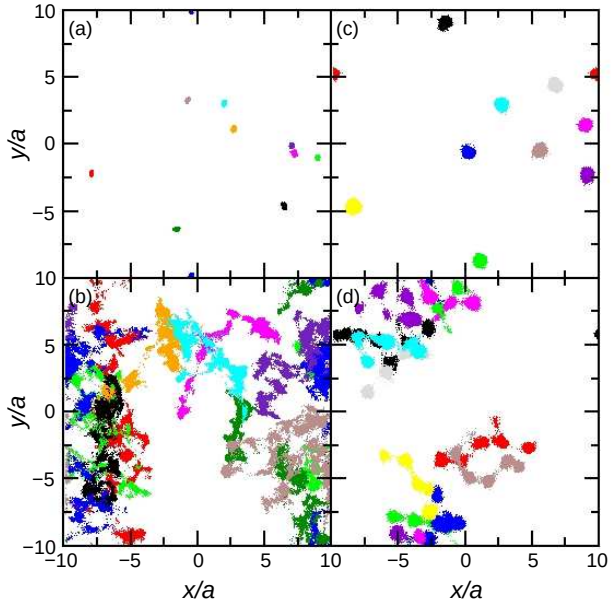

FIG. 4: Representative trajectories of particles whose displacements in the xy-plane over a time interval τ_α are much smaller or much larger in magnitude than average. Particle traces have been projected onto this plane for graphical simplicity. Left panels depict dynamics of a strongly attractive system, $\phi_p = 0.375$. Particles among the 5% least mobile are shown in (a), while particles among the 5% most mobile are shown in (b). Right panels correspond to a weakly attractive system, $\phi_p = 0.05$. Again, trajectories exhibiting extremely small displacements (c) are plotted in the top panel. Trajectories exhibiting extremely large displacements (d) are plotted in the bottom panel.

pecially vivid. The limited spatial extent of facilitating defects in a hard sphere glass cuts off the range of available displacements. Clustering of these defects as attractions are introduced provides increasingly extended loose regions for mobile particles to explore. Our numerical results provide strong evidence for segregation of jammed and unjammed regions of attractive liquids at high density. Such segregation is an obvious feature of attractive colloids at low ϕ_c, which form stable (though likely nonequilibrium) gel-like networks. In that case, the spacing between dense regions of the network establishes a minimum length scale for dynamic heterogeneity. It is remarkable that remnants of this behavior persist at high packing fraction, where spatial heterogeneity of liquid structure is subtle.

In summary, the change in dynamics induced by short-ranged attractions in a dense model liquid is dramatic even on the microscopic scale. Our results reveal three distinct regimes of dynamical heterogeneity. For weak attractions, mobilized particles make discrete jumps between cage structures, which may remain correlated over many jump times. For a range of intermediate attraction strengths, Gaussian particle displacement statistics suggest instead very fluid and uniform motion. The role of attractions in this regime, we suggest, is to bind small transient clusters which move on a time scale comparable to their lifetimes. Strong attractions restore some discreteness of particle displacements, presumably because transient clusters are too large to move appreciably on pertinent time scales. We thus conclude that "attractive" glassiness is driven by spatial redistribution of facilitating defects. Although extended loose domains permit large particle displacements, their growth depletes mobility in surrounding areas, which in turn inhibits relaxation of domain interfaces. We are pursuing further calculations to confirm this clustering of mobility in dense environments and to characterize the correlated fluctuations underlying fluidity at intermediate attraction strength.

We would like to thank Laura Kaufman for useful discussions. We acknowledge the NSF (D.R.R.), DOE (P.L.G.), and the United States-Israel Binational Science Foundation (grant number 2002100 to D.R.R and E.R.) for financial support. D.R.R. is a Camille Dreyfus Teacher-Scholar and an Alfred P. Sloan Foundation Fellow.

[1] U. Balucani and M. Zoppi, *Dynamics of the Liquid State* (Oxford, New York, 1994).
[2] W. Kob *et al.*, Phys. Rev. Lett. **79**, 2827 (1997).
[3] C. Donati *et al.*, Phys. Rev. Lett. **80**, 2338 (1998).
[4] D. N. Perera and P. Harrowell, Phys. Rev. E **54**, 1652 (1996).
[5] R. Yamamoto and A. Onuki, Phys. Rev. E **58**, 3515 (1998).
[6] L. A. Deschenes and D. A. Vanden Bout, Science **292**, 255 (2001).
[7] E. V. Russell and N. E. Israeloff, Nature **408**, 695 (2000).
[8] S. A. Reinsberg *et al.*, J. Chem. Phys. **114**, 7299 (2001).
[9] E. R. Weeks *et al.*, Science **287**, 627 (2000).
[10] C. Donati *et al.*, Phys. Rev. E **60**, 3107 (1999).
[11] S. Butler and P. Harrowell, J. Chem. Phys. **95**, 4454 (1991).
[12] J. P. Garrahan and D. Chandler, Proc. Nat. Acad. Sci. **100**, 9710 (2003).
[13] J. P. Garrahan and D. Chandler, Phys. Rev. Lett. **89**, 035704 (2002).
[14] S. Whitelam, L. Berthier, and J. P. Garrahan, Phys. Rev. Lett. **92**, 185705 (2002).
[15] S. Whitelam and J. P. Garrahan, Facilitated spin models in one dimension: a real-space renormalization group study, cond-mat/0405647.
[16] M. Vogel and S. C. Glotzer, Temperature dependence of spatially heterogeneous dynamics in a model of viscous silica, cond-mat/0404733.
[17] L. Berthier and J. P. Garrahan (unpublished).
[18] K. Dawson *et al.*, Phys. Rev. E **63**, 011401 (2001).
[19] A. M. Puertas, M. Fuchs, and M. E. Cates, Phys. Rev. Lett. **88**, 098301 (2002).
[20] A. M. Puertas, M. Fuchs, and M. E. Cates, Phys. Rev. E **67**, 031406 (2003).

[21] L. Fabbian *et al.*, Phys. Rev. E **59**, R1347 (1999).
[22] K. N. Pham *et al.*, Science **296**, 104 (2002).
[23] The effect of such a term on the type of heterogeneous motion discussed here has not been unambiguously demonstrated. Nor is it clear that such a repulsion exists between colloidal particles studied in experiments.
[24] M. E. Cates *et al.*, Theory and simulation of gelation, arrest and yielding in attracting colloids, cond-mat/0403684.
[25] T. B. Schroder, S. Sastry, J. C. Dyre, and S. C. Glotzer, J. Chem. Phys. **112**, 9384 (2000).
[26] R. Yamamoto and A. Onuki, Phys. Rev. Lett. **81**, 4915 (1998).
[27] R. K. Murarka and B. Bagchi, Phys. Rev. E **67**, 051504 (2003).
[28] D. R. Reichman, E. Rabani, and P. L. Geissler (unpublished).
[29] E. J. Gumbel, *Statistics of Extremes* (Columbia University Press, New York, 1958).
[30] P. L. Geissler and D. R. Reichman, Short-ranged attractions in jammed liquids: How cooling can melt a glass, cond-mat/0402673.
[31] After this work was submitted to the Los Alamos archive server, we became aware of related work in press by Puertas, Fuchs and Cates (which appeared as J. Chem. Phys. 121, 2813 (2004)). That work also confirms the earlier central ideas contained in the theory of Geissler and Reichman (cond-mat/0402673). Their conclusions differ from those presented in this paper in that they view the bimodal distribution of particle displacements as indicative of a form of dynamical heterogeneity unique to systems with attractive interactions. We contend that this bimodality is generic to glassy systems. The study of Puertas et al. further differs from our own in focusing on a much lower volume fraction, for which there is no corresponding repulsive glassy state to compare. It is interesting that much of the behavior they reported exists even at the very high volume fractions studied here.